Atmospheric Research 248 (2021) 105153

Contents lists available at ScienceDirect

Atmospheric Research

journal homepage: www.elsevier.com/locate/atmosres

Estimated contribution of vehicular emissions to carbonaceous aerosols in urban Beijing, China

Yang Cui[a,b], Wan Cao[a,b], Dongsheng Ji[a,b,c,*], Wenkang Gao[a], Yuesi Wang[a,b,c]

[a] State Key Laboratory of Atmospheric Boundary Layer Physics and Atmospheric Chemistry, Institute of Atmospheric Physics, Chinese Academy of Science, Beijing 100191, China

[b] University of Chinese Academy of Sciences, Beijing 100049, China

[c] Center for Excellence in Regional Atmospheric Environment, Institute of Urban Environment, Chinese Academy of Science, Xiamen, 361021, China

ARTICLE INFO

Keywords:
Organic carbon
Elemental carbon
Source apportionment
Nighttime
Urban Beijing
Vehicle emissions

ABSTRACT

Worldwide attention has been focused on air pollution associated with vehicle emissions. With the highest number of vehicles, Beijing has experienced air pollution related to vehicle emissions. To better recognize the contributions of vehicle emissions to organic carbon (OC) and elemental carbon (EC), hourly measurements of OC and EC in $PM_{2.5}$ were conducted in urban Beijing from June 1, 2016 to May 31, 2017 in addition to auxiliary measurements of water-soluble ions and elements. The average concentrations of OC and EC were 11.9 ± 11.1 and 3.7 ± 3.6 μg/m^3 during the study period, respectively, while those of OC and EC during the nighttime (0:00–6:00), morning rush hour (7:00–9:00) and evening rush hour (17:00–19:00) were 12.9 ± 12.9 μg/m^3 and 4.4 ± 4.3 μg/m^3, 10.4 ± 9.8 μg/m^3 and 3.7 ± 3.1 μg/m^3, and 12.3 ± 8.7 μg/m^3 and 3.5 ± 2.4 μg/m^3, respectively. The diurnal variations in OC and EC concentrations showed higher values during the nighttime, morning rush hour and evening rush hour. Strong correlations were found between OC and CO (r^2 = 0.76–0.79) and between OC and NO_x (r^2 = 0.63–0.68); strong correlations were also found between EC and CO (r^2 = 0.76–0.81) and between EC and NO_x (r^2 = 0.63–0.68) during the nighttime, morning rush hour and evening rush hour. The results of source apportionment based on the hourly $PM_{2.5}$-associated chemical composition by a positive matrix factorization model showed that vehicle emissions accounted for 23.0% of $PM_{2.5}$. From the profiles of the source apportionment of $PM_{2.5}$, it could be found that vehicle emissions contributed 51.2%, 51.3% and 25.2% of the concentrations of OC, EC and $PM_{2.5}$ on average during the nighttime, respectively. The contributions of vehicle emissions to OC, EC and $PM_{2.5}$ during the nighttime were higher than or close to those during the evening rush hour and the morning rush hour. This result indicated that vehicular emissions play an important role in carbonaceous aerosols and $PM_{2.5}$ during the nighttime. The above results provide insight into the quantitative evaluation of the contribution of vehicular emissions to OC, EC and $PM_{2.5}$ and thus could provide references for pollution control in areas with high vehicular emissions.

1. Introduction

With the rapid development of the economy, urbanization and industrialization in China over the past decades, particulate matter (PM) pollution has become a serious air pollution issue (Gao et al., 2017; Pui et al., 2014). As a major chemical component of PM, carbonaceous aerosols consist primarily of organic and elemental carbon (OC and EC, respectively) (Chang et al., 2017; Ji et al., 2019b), which are closely related to fuel combustion (Sun et al., 2018; Zhang et al., 2015). Studies on the evolution and source of carbonaceous aerosols have been helpful for further mitigating $PM_{2.5}$ pollution (Chang et al., 2017; Ji et al., 2019b). Moreover, carbonaceous aerosols play an important role in climate change and public health risks. OC and EC can influence Earth's radiation balance directly and indirectly (Bond et al., 2013). Visibility degradation is also related to the increased concentrations of OC and EC (Huang et al., 2012). Polycyclic aromatic hydrocarbons (PAHs) that are rich in OC pose a possible health hazard to humans (Li et al., 2016b). EC results in adverse effects in humans because it carries PAHs and heavy metals, and EC is closely related to the risk of cardiovascular conditions (Biswas et al., 2009). Therefore, the study of OC and EC has attracted worldwide attention to due to their influence on the environment, human health and climate.

* Corresponding author at: State Key Laboratory of Atmospheric Boundary Layer Physics and Atmospheric Chemistry, Institute of Atmospheric Physics, Chinese Academy of Science, Beijing 100191, China.

E-mail address: jds@mail.iap.ac.cn (D. Ji).

https://doi.org/10.1016/j.atmosres.2020.105153
Received 24 May 2020; Received in revised form 18 July 2020; Accepted 20 July 2020
Available online 23 July 2020

In response to environmental, health and climate concerns, numerous studies have focused on spatiotemporal variations and potential source areas of OC and EC and the estimation of secondary OC (SOC) (Chang et al., 2017; Lin et al., 2009; Wu et al., 2019; Yao et al., 2020; Zhao et al., 2013). In addition, previous studies have used different methods to apportion the sources of OC and EC in $PM_{2.5}$. For example, receptor models have been used for identifying sources of OC (Belis et al., 2013), while the light absorption coefficient method, receptor models, the macro-tracer method, the radiocarbon method, isotopic ratios and air quality models have been used for apportioning EC sources (Briggs and Long, 2016; Zhao et al., 2018). The above methods have been widely used for apportioning the sources of OC and EC. However, limited by data with high temporal resolution, the dynamic evolution of the sources during specific periods has not been quantitatively obtained. Vehicle emissions have been identified as an important source of OC and EC in urban areas (Wong et al., 2019). Due to the significant contribution of vehicle emissions to OC and EC, knowledge of quantitative traffic-related contributions are vital for policymakers or researchers to develop mitigation measures, improve air quality and reduce the uncertainty concerning OC and EC emissions (Huang et al., 2014; Wong et al., 2019).

Beijing, one of the core cities in the Beijing-Tianjin-Hebei region (the most highly polluted area in the world), had a vehicle population of 6.1 million in 2018. To reduce traffic congestion and control air pollutant emissions, the Beijing Municipal Government has implemented a series of control measures, such as allowing heavy-duty vehicles (HDVs) and heavy-duty diesel trucks (HDDTs) into the 5th Ring Road only from 0:00 to 6:00 (local time) every day. Despite these measures, the results recently published by the Beijing Municipal Ecology and Environment Bureau showed that mobile sources still contributed 45% to $PM_{2.5}$. Although vehicular emissions play a very important role in $PM_{2.5}$, previous results regarding the quantitative contributions of vehicular emissions to OC and EC are inadequate due to complicated analysis processes such as the accurate analysis of organic species associated with $PM_{2.5}$ or radiocarbon and carbon isotope signatures (Hu et al., 2010; Zhang et al., 2015; Zhang et al., 2009; Zheng et al., 2006). It can be seen that a simple and efficient method is necessary and urgent to estimate the contribution of vehicular emissions to OC and EC.

In Beijing there are three important periods of vehicular emission: morning and evening rush hours as well as nighttime emissions of HDVs and HDDTs. To the best of our knowledge, no quantitative contribution of vehicular emissions to OC and EC has been estimated during the periods of intensive vehicular emission. From the above background, hourly OC and EC concentrations in $PM_{2.5}$ were measured from June 1, 2016, to May 31, 2017, in a typical urban environment of Beijing. The variations and characteristics of OC and EC were analyzed during the traffic-related periods. Based on the source apportionment profiles obtained from hourly observations, the contributions of vehicular emissions to OC, EC and $PM_{2.5}$ were quantitatively evaluated during the nighttime (0:00–6:00), morning rush hour (7:00–9:00) and evening rush hour (17:00–19:00). These results provide an example of applying highly time-resolved data to identify the contribution of pollution sources and serve as a reference for controlling air pollution associated with vehicular emissions in developing countries.

2. Instruments and measurements

2.1. Sampling site

As shown in Fig. 1, the sampling site (39.98° N, 116.38° E, 44 m above ground) as established at the subcenter of the Institute of Atmospheric Physics (IAP), the Chinese Academy of Sciences (CAS), which is spatially representative (Sun et al., 2018). The site was located between the 3rd ring road and 4th ring road in the urban area. According to previous studies (Ji et al., 2016b; Sun et al., 2018; Xu et al., 2019b), the sampling site was selected as a typical urban site and was affected by local emissions, including traffic and a variety of residential sources. The linear regression relationship of $PM_{2.5}$ concentrations between our sampling site and other sites of the Ministry of Ecology and Environment of the People's Republic of China in Beijing for 2017 was analyzed. As seen in Table S1, except for Huairou, the $PM_{2.5}$ concentrations at other sites showed exhibited a higher correlation with our sample site ($r^2 > 0.8$), thus the sampling site better represented the urban area of Beijing. This sampling site was surrounded by roadways including being 1.2 km north of the 3rd Ring Road, 200 m north of the Beitucheng West Road, 200 m east of JiangZang Highway, 1 km west of Beitaipingqiao Road and 2 km south of the North 4th Ring Road. The daily vehicle fleet amount was 229.4 thousand, and the annual average speeds of vehicles were 27.8 and 24.6 km/h in the morning and evening rush hour in 2016, respectively (http://www.bjtrc.org.cn/List/index/cid/7.html). No industrial sources were near the sampling site. The observation period was from June 1, 2016 to May 31, 2017. The sampling devices were installed on the roof of a two-story building (10 m above the ground).

2.2. Instrumentation

Semi-continuous OC/EC analyzers (Model 4, Sunset Laboratory Inc. OR, USA) were used to measure hourly OC and EC concentrations with a 2.5 μm aerodynamic diameter cut-point cyclone. The sampling flow rate was 8 L/min. The ambient sample were collected for 40 min, the analytical process was performed in 15 min, and then a 5 min instrument-stabilizing process was performed. Volatile organic compounds were removed using a carbon-impregnated parallel plate organic denuder installed on the analyzer. An internal standard CH_4 mixture (5.0%; ultrahigh purity He) was automatically injected to calibrate the analyzer at the end of every analysis. In addition, off-line calibration was conducted every 3 months with an external amount of sucrose standard (1.06 μg). Detailed information about this equipment can be found in the literature (Ji et al., 2019b).

$PM_{2.5}$-associated water-soluble inorganic ions including SO_4^{2-}, NH_4^+, NO_3^-, Ca^{2+}, Na^+, Mg^{2+}, F^+ and K^+, were monitored hourly using an ambient ion monitor (Model URG 9000D, URG Corp., USA). The operational principle and more detailed information on the ambient ion monitor can be found in the literature (Liu et al., 2017b). Before each measurement period, the sampling flow was calibrated, and calibrated curves of the instrument were constructed. The correlation coefficients were ≥ 0.999 for individual species.

The hourly concentrations of 23 elements in $PM_{2.5}$ were simultaneously measured using an automated multi-metal monitor (Xact 625, Cooper Environmental Services, USA), including K, V, Ca, Cu, Cr, Ag, As, Ba, Zn, Mn, Fe, Ni, Se, Ga, Co, Cd, Sn, Sb, Au, Hg, Tl, Pb and Pd. Detailed information on this instrument can be found in Cui et al. (2020). K, Ca, Cr, V, Cu, Fe, Mn, Ni, Zn, As, Se, Ba and Pb were used for the source apportionment of $PM_{2.5}$ in this study.

CO, O_3 and NOx were measured by a gas filter correlation non-dispersive infrared analyzer (model 48I, Thermo-Fisher (TE), USA), an ultraviolet photometric analyzer (model 49I, TE, USA) and a chemiluminescence analyzer (model 42I, TE, USA). A synchronized hybrid ambient real-time particulate monitor (model 5030, TE, USA) was used to measure $PM_{2.5}$ during the entire campaign. Quality assurance and control (QA/QC) of all aspects of the instrumentation in this section can be found in the Supporting Information.

2.3. PMF model

The US EPA positive matrix factorization (PMF) 5.0 model is a multivariate factor analysis model and has been widely used for $PM_{2.5}$ source apportionment (Gao et al., 2016; Liu et al., 2019). The PMF model decomposes the data matrix X into a source profile matrix (F) and a source contribution matrix (G) (Paatero and Tapper, 1994). The

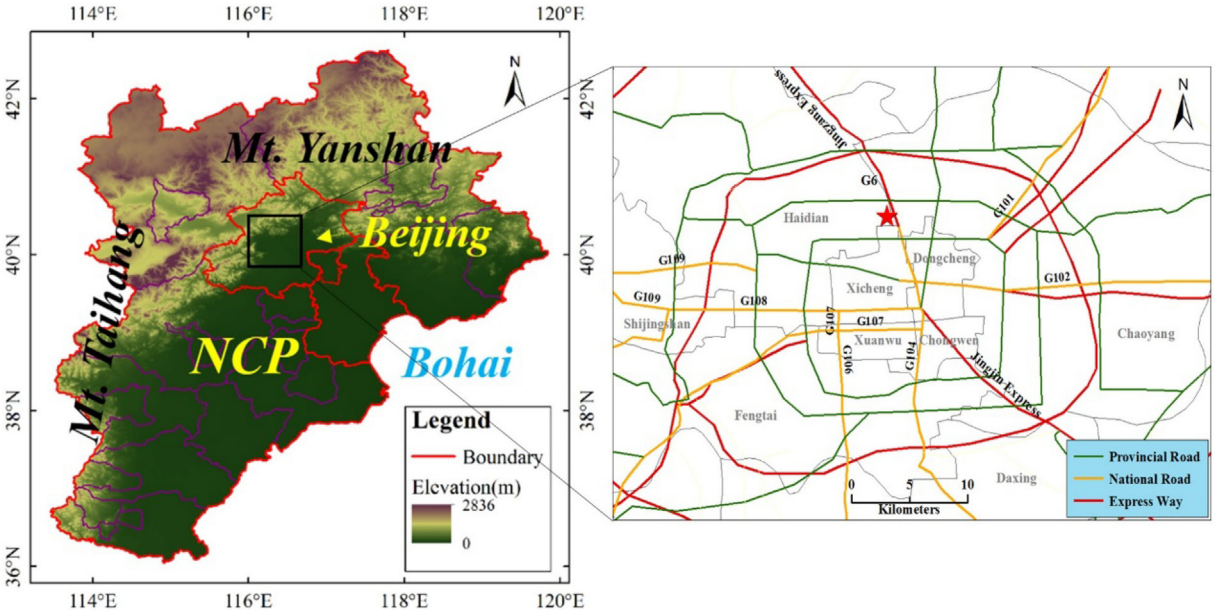

Fig. 1. Geographical location of the sampling site (the red star represents the location of the sampling site).

goal of receptor modes is to solve the following equation:

$$X_{ij} = \sum_{k=1}^{p} g_{ik} f_{ij} + e_{ij} \quad (1)$$

where X_{ij} represents the j^{th} species measured concentration in the i^{th} sample, g_{ik} represents the k^{th} source contribution to the i^{th} sample, and f_{kj} represents the j^{th} chemical profile from the k^{th} source. Here, p represents the number of factors, and e_{ij} represents the residual of each species. Minimizing the objective function Q (Eq. (2)) can solve Eq. (1) with PMF and obtain factor contributions and profiles:

$$Q = \sum_{i=1}^{n} \sum_{j=1}^{m} \left[\frac{X_{ij} - \sum_{K=1}^{P} g_{ik} f_{kj}}{u_{ij}} \right]^2 \quad (2)$$

where u_{ij} represents the uncertainty of each sample/species, which is applied to weight any dataset that contains missing data, data below the method detection limit (MDL), outliers and sampling errors. The input data for PMF runs include the concentration and uncertainty of each sample. The high time-resolution $PM_{2.5}$ chemical composition dataset includes hourly OC, EC, water-soluble inorganic ions (SO_4^{2-}, NO_3^-, NH_4^+, Cl^-) and elements (K, Ca, V, Cr, Mn, Fe, Ni, Cu, Zn, As, Se, Ba, and Pb). The MDLs of measured species in $PM_{2.5}$ are shown in Table S2. Species with more than 50% of measured concentrations below the MDL were removed. Higher MDLs of Ca^{2+} and K^+ resulted in higher percentages of Ca^{2+} and K^+ below the MDLs than Ca and K. Thus, Ca and K were used in this study. Although more than 50% of V concentrations were below the MDL, because V is an important tracer of oil combustion, this element was retained to aid in the source analysis (Cui et al., 2019). Finally, a total of 18 variables (OC, EC, SO_4^{2-}, NO_3^-, NH_4^+, Cl^-, K, Ca, V, Cr, Mn, Fe, Cu, Zn, Ni, As, Se, Ba and Pb) were used in the PMF model. In this study, $PM_{2.5}$ was set as the total variable. July 1–31, 2016, November 8–30, 2016, December 1–31, 2016 and April 1–30, 2017 were selected to represent summer, autumn, winter and spring, respectively. Missing data were replaced by the median. The uncertainty can be calculated using a fixed fraction of the MDL provided if the concentration of the sample data is less than or equal to the MDL, which is expressed as follows:

$$U = \frac{5}{6} \times MDL \quad (3)$$

When the concentration of the sample is greater than the MDL, the uncertainty can be calculated by:

$$U = \sqrt{(error\ fraction \times concentration)^2 + (0.5 \times MDL)^2} \quad (4)$$

By analyzing the Q values, the goodness of PMF fit, the distribution of the scaled residuals and the G-space plot can help identify the optimal number of factors, including suitable factor profiles and contributions with physical meanings. Displacement (DISP) and bootstrapping (BS) were used to estimate the uncertainty of the PMF solution.

2.4. Statistical analyses

Nonparametric tests, such as the Mann-Whitney U test, Kruskal-Wallis rank sum test and the Dunn multiple-comparison test were applied to assess whether the differences in the species/parameter data were statistically significant. The statistical analyses were performed with R (Teetor, 2011), and the significance was set at $p < .05$.

3. Results and discussion

3.1. OC and EC concentrations

The annual average concentrations of OC and EC were 11.9 ± 11.3 and 3.7 ± 3.6 μg/m^3, respectively, which accounted for 15% and 4.5% of $PM_{2.5}$. The concentrations of OC and EC in different months and seasons during the study period are shown in Fig. 2. As shown in Fig. 2, OC and EC had obvious seasonal variations with higher levels in winter (19.0 and 5.5 μg/m^3) and autumn (11.8 and 4.3 μg/m^3) and lower levels in spring (9.3 and 2.6 μg/m^3) and summer (7.3 and 2.5 μg/m^3). The seasonal variations in OC and EC are closely related to emission intensities and meteorological conditions (Ji et al., 2016b). Increased OC and EC levels in winter were attributed to the increased emission for heating and unfavorable meteorological conditions (low atmospheric temperature (*T*), wind speed (*WS*) and planetary boundary layer (*PBL*) height (Fig. S1)). In contrast, lower emissions, higher *T*, favorable dilution conditions and frequent wet scavenging processes in summer resulted in the lowest concentrations of OC and EC. The concentrations of OC and EC in this study were compared with those published in China and other countries. Table 1 lists recently published results for the concentrations of OC and EC in cities in China and other countries. As shown in Table 1, the concentrations of OC and EC in Beijing were higher than those in Paris, France (Bressi et al., 2013); Seoul, South

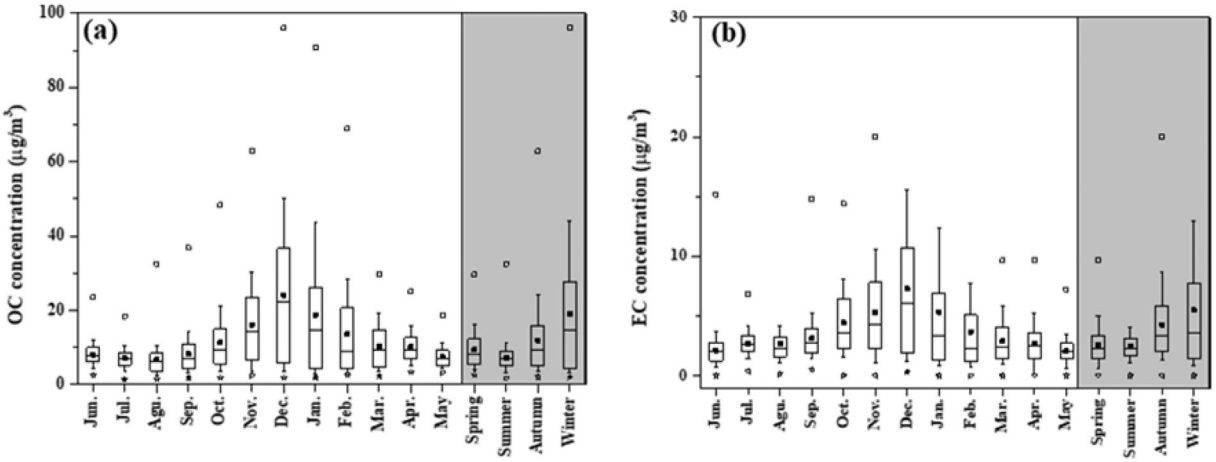

Fig. 2. The 1-h OC (a) and EC (b) concentrations in individual sampling months in Beijing during the study period from June 2016 to May 2017. (box length: 25th and 75th percentiles; whiskers: 10th and 90th percentiles; square in the box: mean; line in the box: median; asterisk: minimum values; hollow square: maximum values).

Korea (Park et al., 2019); Toronto, Canada (Sofowote et al., 2014); and Shanghai (Chang et al., 2017), Guangzhou (Tao et al., 2017), Tianjin (Ji et al., 2019a) and Lhasa (Li et al., 2016a) in China. However, the concentrations of OC and EC were than lower those in New Delhi, India (Sharma and Mandal, 2017); Bangkok, Thailand (Pongpiachan et al., 2015); and Shijiazhuang (Ji et al., 2019a), Tangshan (Ji et al., 2019a), Xi'an (Wang et al., 2015b), Lanzhou (Wang et al., 2016b), Heze (Liu et al., 2017a), and Chongqing (Chen et al., 2017) in China. For some cities, such as Hongkong, China (Huang et al., 2014), Istanbul, Turkey (Flores et al., 2020); and São Paulo, Brazil (Pereira et al., 2017), the concentrations of OC in these cities were lower than those in this study, while the concentrations of EC were higher. Although obvious difference or similarity in OC and EC concentrations was observed in cities of China and other countries, studies were insufficient on characterization of OC and EC during peak traffic periods. The levels of OC and EC and correlation between OC and EC and CO and NOx will be discussed during peak traffic periods in detail in the following section.

3.2. Diurnal variations in OC and EC in Beijing

As shown in Fig. 3, diurnal variations in OC and EC concentrations were observed in the four seasons in Beijing. To further discuss the effects of vehicle emissions on OC and EC, diurnal variations in CO and NO_x are also shown. In addition to higher concentrations during the morning rush hour (MR, 7:00–9:00) and evening rush hour (ER, 17:00–19:00), EC also showed higher values during the nighttime (00:00–06:00). Strong correlations were found between EC and CO (r^2 = 0.76–0.81, $p < .05$) and between EC and NOx (r^2 = 0.63–0.68, $p < .05$) during the nighttime, MR and ER. Various emission sources for NOx and the higher reactivity of NOx during the daytime (06:00–23:00) resulted in a weaker correlation between EC and NOx (r^2 = 0.62, $p < .05$) than between EC and CO (r^2 = 0.75, $p < .05$). The concentrations of OC also showed higher values during the nighttime, MR and ER than at other times. An additional peak in the OC concentration occurred at approximately 12:00, accompanied by the peak OC/EC value (Fig. 5). Strong correlations were also found between OC and CO (r^2 = 0.76–0.79, $p < .05$) and between OC and NOx (r^2 = 0.63–0.68, $p < .05$) during the nighttime, MR and ER. Based on the emission inventory of CO and NO_x (Liu et al., 2018), both mainly originated from vehicular emissions. This result also suggests that vehicle emissions play an important role in OC and EC. The average EC concentrations during the nighttime were higher than those during MR and ER. A previous study performed in Beijing (Yan et al., 2014) showed that the vehicle flow is 20,000/h during traffic rush hours,

Table 1
Comparison of the average concentrations (μg/m³) of OC and EC in several cities in China and other countries.

Sampling location	Site type	Period	Method	OC	EC	Reference
Beijing, China	Urban	Jun. 2016-May 2017	TOT	11.9	3.7	This study
Shanghai, China	Urban	Jan. 2014-Dec. 2014	TOT	7.8	2.1	Chang et al. (2017)
Tianjin, China	Urban	Dec. 2016-Nov. 2017	TOT	12.0	3.1	Ji et al. (2019a)
Shijiazhuang, China	Urban	Dec. 2016-Nov. 2017	TOT	22.8	5.4	Ji et al. (2019a)
Tangshan, China	Urban	Dec. 2016-Nov. 2017	TOT	12.1	9.6	Ji et al. (2019a)
Xi'an, China	Urban	2010	TOR	21.8	6.1	Wang et al. (2015b)
Guangzhou, China	Urban	2014–2015	TOR	8.2	4.0	Tao et al. (2017)
Lanzhou, China	Urban	Jan. to Dec., 2014	TOR	17.7	9.0	Wang et al. (2016b)
Heze, China	Urban	Agu. 2015 to Apr. 2016	TOR	15.9	6.2	Liu et al. (2017a)
Chongqing, China	Urban	May 2012 to May 2013	TOT	14.5	4.0	Chen et al. (2017)
Lhasa, China	Urban	May 2013 to Mar. 2014	TOR	3.3	2.2	Li et al. (2016a)
Hong Kong, China	Roadside	May 2011 to April 2012	TOT	7.8	4.4	Huang et al. (2014)
Istanbul, Turkey	Urban	Jan. 2017-Jan. 2018	TOT	11.3	4.1	Flores et al. (2020)
Bangkok, Thailand	Urban	Nov. 2010-Jan. 2012	TOR	18.8	6.7	Pongpiachan et al. (2015)
Seoul, Korea	Urban	Jan. 1, 2013 to Dec. 31, 2014	TOT	4.1	1.8	Park et al. (2019)
New Delhi, India	Urban	Jan. 2013 to May 2014	TOR	17.7	10.3	Sharma and Mandal (2017)
Pairs, France	Urban	Sep. 2009 to Sep. 2010	TOT	3.0	1.4	Bressi et al. (2013)
Toronto, Canada	Urban	Dec. 2010 to Nov. 2011	TOT	3.4	0.5	Sofowote et al. (2014)
São Paulo, Brazil	Urban	2014	TOT	10.2	7.0	Pereira et al. (2017)

TOR: thermal-optical reflectance; TOT: thermal-optical transmittance.

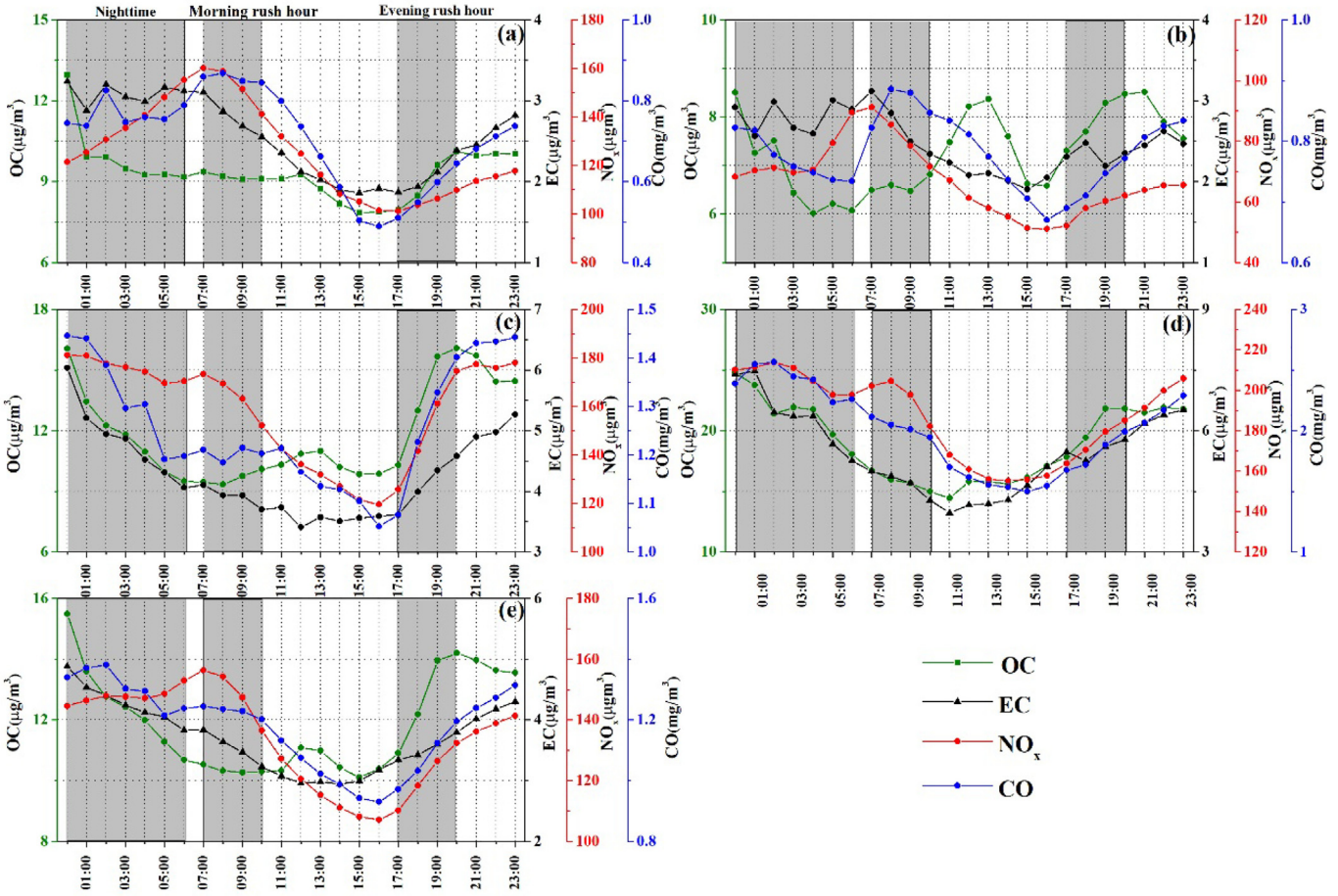

Fig. 3. Diurnal variations in OC, EC, NOx and CO concentrations in (a) spring, (b) summer, (c) autumn, (d) winter and (e) year round. The three shaded areas represent the three periods of nighttime, morning rush hour and evening rush hour.

while the flow is only approximately 2000/h during the nighttime on North 4th Ring Road. Of the vehicle flow, 17.7% is HDVs and HDDVs during the nighttime. However, the emission factors of OC and EC emitted from HDVs and HDDVs are approximately 12–108 times higher than those emitted from gasoline vehicles (Yang et al., 2019). Hence, higher EC concentrations during the nighttime may be closely associated with emissions from HDVs and HDDVs.

To study the influence of HDVs and HDDTs emissions on the concentrations of OC and EC, comparisons of the concentrations of OC and EC during the MR, ER and nighttime are shown in Fig. 4. As shown in Fig. 4(a) and (b), obvious differences in OC and EC concentrations were found during the MR, ER and nighttime. On the annual average, the concentrations of OC during the nighttime were 24.0% and 4.9% higher than those during the MR and ER, respectively, while those of EC were 18.9% and 25.7% higher than those during the MR and ER, respectively. The difference in OC concentrations during the ER and nighttime was not significant ($p > .05$, Mann-Whitney U test). Seasonally, the concentrations of EC during the nighttime were 55.0%, 21.7%, 25.0% and 22.2% higher than those during the ER for spring, summer, autumn and winter, respectively, while they were 6.9%, 25.0% and 34.7% higher than those during the MR for spring, autumn and winter, respectively. In contrast to the concentrations of EC, the concentrations of OC during the nighttime were 9.8%, 7.7%, 30.5% and 37.9% higher than those during the MR for spring, summer, autumn and winter, respectively, while they were 16.1% and 12.7% higher than those during the ER in spring and winter, respectively. Based on the Mann-Whitney U test, the differences in the concentrations of OC during the nighttime and the MR in summer and during the nighttime and the ER in autumn and winter were not significant ($p > .05$), while the differences in the concentrations of EC during the nighttime and the MR in summer and during the nighttime and the ER in winter were not significant ($p > .05$).

To exclude meteorological influences on the evolution of OC and EC, the values of OC/ΔCO (ΔCO = CO-$CO_{background}$, where $CO_{background}$ is the background concentration of CO and is calculated as the average of the lowest 10th percentile of the CO mixing ratios observed during the entire study period) and EC/ΔCO were calculated during the MR, ER and nighttime (Ji et al., 2019a). On the annual average, the values of OC/ΔCO during the nighttime were 25.6% higher than those during the MR, while the values of EC/ΔCO were 18.4% and 3.6% higher than those during the MR and ER, respectively. The values of OC/ΔCO during the nighttime were 24.3% lower than those during the ER. There was no significant difference in the values of EC/ΔCO during the nighttime and the ER ($p > .05$). Seasonally, the values of OC/ΔCO during the nighttime were 30.1%, 26.7%, 19.8% and 22.9% higher than those during the MR but 22.7%, 19.7%, 25.6% and 31.4% lower than those during the ER for spring, summer, autumn and winter, respectively ($p < .05$). The values of OC/ΔCO during the nighttime were lower than those during the ER, which was probably caused by a combination of cooking emissions and secondary formation. Cooking-related emissions and the secondary formation of OC are characterized by a large amount of OC but little or no EC (Zhang et al., 2017; Zhao et al., 2019). Although more OC originates from nighttime HDDV emissions than from gasoline vehicles in the evening, cooking-related emissions and the secondary formation of OC offset the influence of nighttime HDDV emissions. A previous study showed that prevailing southerly winds result in increased secondary pollutants including sulfate and organic matter in Beijing in the late afternoon and evening

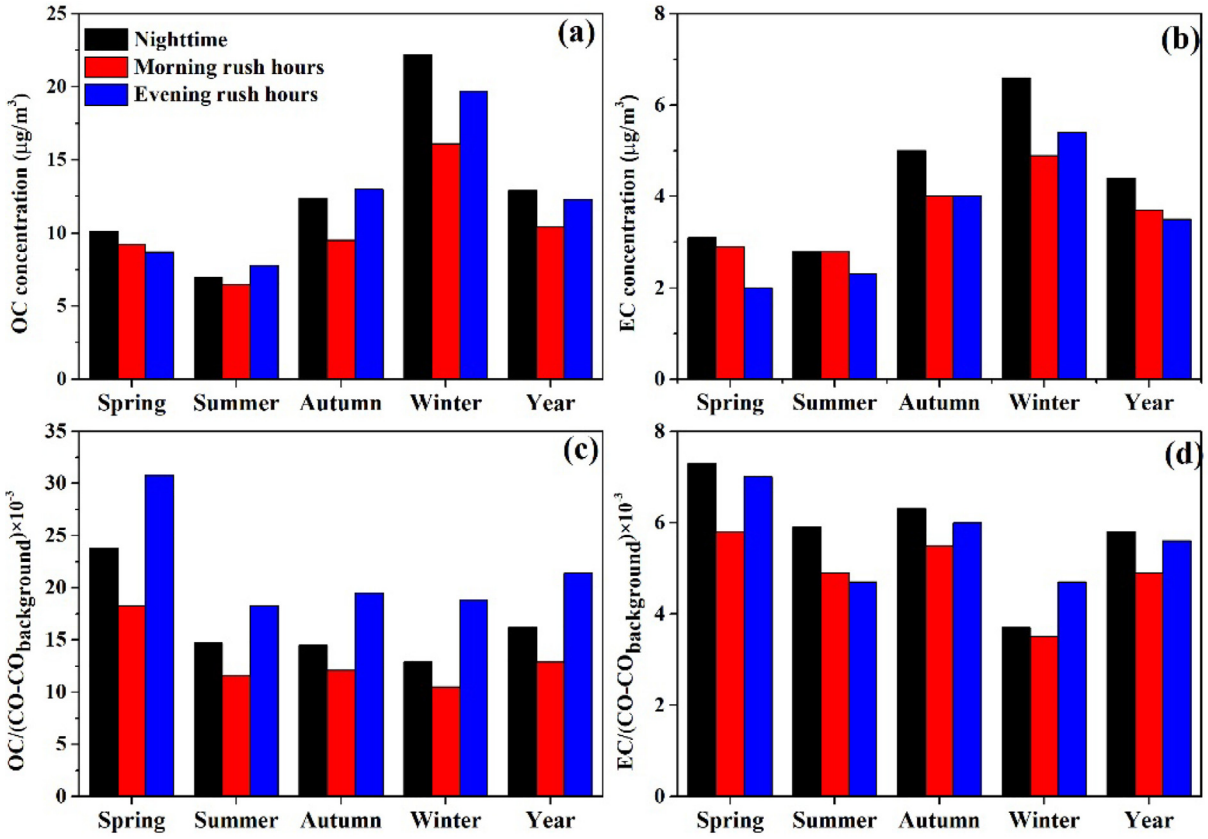

Fig. 4. Average OC (a), EC (b), OC/ΔCO (ΔCO = CO-$CO_{background}$) (c) and EC/ΔCO (d) during the nighttime, morning rush hours and evening rush hours in the four seasons. The background value of CO was calculated as the average of the lowest 10th percentile of the CO mixing ratios observed during the entire study period.

(Ji et al., 2016a). The synergistic effect of cooking activities and the secondary formation of OC may explain the higher values of OC/ΔCO during the ER (Park et al., 2008). As shown in Fig. 4(d), the EC/ΔCO values during the nighttime were 25.9%, 20.4%, 14.5% and 5.7% higher than those during the MR for spring, summer, autumn and winter, respectively, while they were 4.3%, 25.5% and 5.0% higher than those during the ER hour in spring, summer and autumn, respectively. Surprisingly, in the winter, EC/ΔCO during the nighttime was 21.3% lower than that during the ER. A possible reason for the above difference is the increase in the ΔCO values related to the enhancement in emissions from vehicle exhaust at low temperatures during the nighttime (Han et al., 2009). Notably, the differences in the values of EC/ΔCO during the nighttime and the MR in winter and during the nighttime and the ER in spring and autumn were not significant ($p > .05$).

The diurnal patterns of the OC/EC ratio showed two peaks (Fig. 5). The peaks were observed at approximately 12:00 and 19:00. The peaks of OC recorded at approximately 12:00 were related to photochemical reactions and atmospheric dilution conditions (Chang et al., 2017). Ground-level ozone is associated with atmospheric oxidation capacity. As shown in Fig. S2, the diurnal variation in O_3 showed that O_3 concentrations increased from 7:00 and peaked at approximately 13:00–15:00. Based on the peaks of OC/EC and the diurnal variation in O_3, it could be inferred that the additional peak of OC concentrations was related to photochemical reactions (Chang et al., 2017). The peaks observed at 19:00 were related to a combined effect of vehicular emissions, cooking emissions and the secondary formation of OC. Significant differences in the ratios of OC and EC were observed between the daytime (3.8 ± 2.7) and nighttime (3.0 ± 1.1) ($p < .05$ from the Mann-Whitney U test). The OC/EC ratios vary from 0.22 to 0.93 for diesel engine exhaust and 1.2 to 4.8 for gasoline exhaust (Wu et al., 2016; Hao et al., 2019; Yang et al., 2019). It is obvious that the OC/EC ratios in diesel-power vehicles are lower than those in gasoline-powered vehicles. The emission of gasoline vehicles combined with the photochemical formation of SOC resulted in a higher OC/EC during the daytime than during the nighttime. The average OC/EC ratio during the nighttime (3.0 ± 1.1) was 40% lower than 4.2 ± 3.7 during the ER ($p < .05$). Surprisingly, the average OC/EC ratio (3.0 ± 1.8) during the MR (7:00–9:00) was almost the same as that (3.0 ± 1.1) during the nighttime.

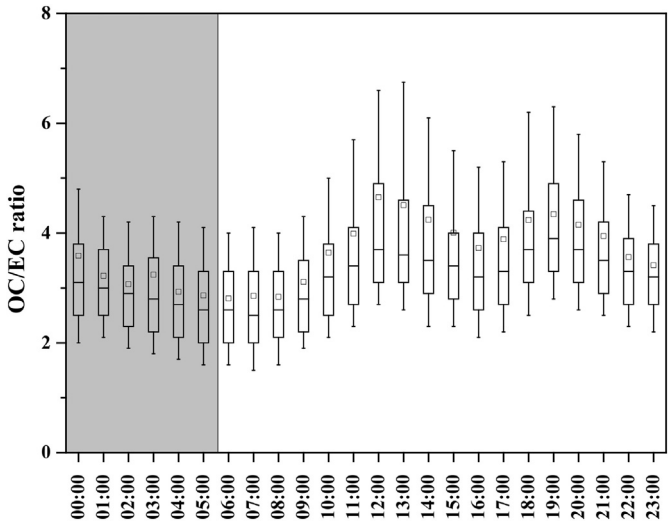

Fig. 5. Diurnal profile of OC/EC ratios from June 2016 to May 2017 (the shaded area represents the nighttime). (box length: 25th and 75th percentiles; whiskers: 10th and 90th percentiles; square in the box: average; line in the box: median).

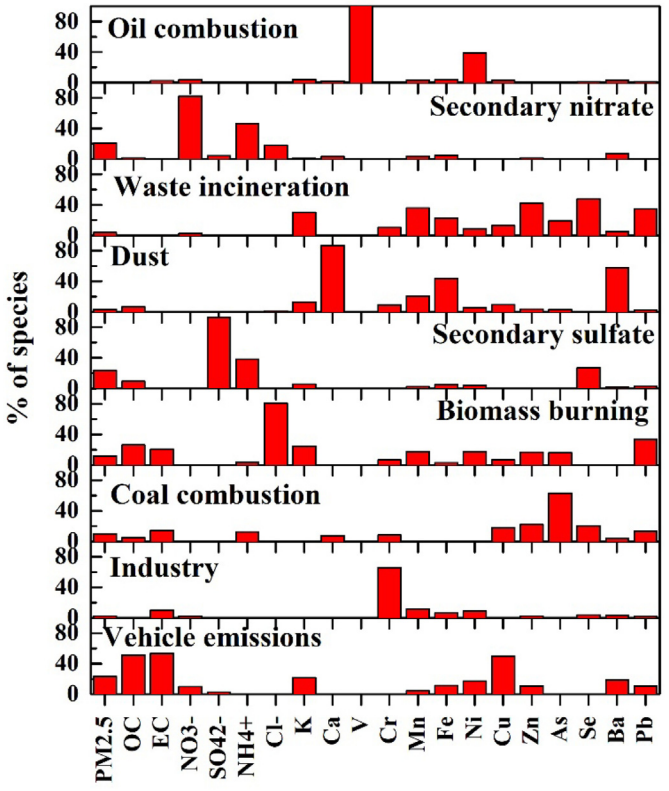

Fig. 6. Source profiles (% of species total) identified by the PMF model.

3.3. Source apportionment of $PM_{2.5}$ based on the PMF model

Six to thirteen factors were tested, and the nine-factor solution was found to be optimum, yielding reasonable source profiles. However, approximately 7.2% of EC was apportioned in secondary nitrate and sulfate. Here, we used the "set to zero" function in the PMF version 5.0 model to constrain EC in the secondary nitrate and sulfate. In contrast to the base run, this constraint caused a 1% increase in the *Q* value. The source profiles identified are shown in Fig. 6. The predicted concentrations of OC, EC and $PM_{2.5}$ were consistent with those observed (Fig. S3). Error estimations for the PMF solution were performed via DISP and BS. As shown in Tables S3 and S4, no swaps occurred in the DISP runs, and more than 99% of the BS runs were mapped for all factors. Thus, the results of source apportionment were stable and reliable.

V and Ni greatly contributed to factor 1, and thus, the source could be regarded as oil combustion (Wang et al., 2016c). On average, this source contributed 1.1% of $PM_{2.5}$.

The secondary nitrate factor (factor 2) was identified by the high loading of nitrate and ammonium, and the distributions of ammonium and nitrate in this factor were 47.9% and 93.6%, respectively.

In factor 3, there were high loadings of K, Mn, Fe, Zn, Se and Pb. This factor was identified as waste incineration. Although previous studies regarding the source profile of waste incineration are insufficient, our identified profile is similar to those of previous studies (Xie et al., 2008; Zíková et al., 2016). This factor contributed 3.9% of $PM_{2.5}$.

Factor 4 had high loadings of Ca, Ba and Fe, and thus, the source could be considered a dust source. The source profile of dust in this study is similar to the results reported by Liu et al. (2019) and Li et al. (2017). Based on the source profile of dust, a higher contribution of $PM_{2.5}$ from dust was observed in the spring than in the other seasons (Table 2).

Factor 5 was heavily weighted by SO_4^{2-} and NH_4^+ and a moderate

Table 2
Concentrations (*c*, μg/m^3) and contributions (%) of the identified sources to $PM_{2.5}$, OC and EC in the four seasons.

	Spring						Summer						Autumn						Winter						Year					
	$PM_{2.5}$		OC		EC		$PM_{2.5}$		OC		EC		$PM_{2.5}$		OC		EC		$PM_{2.5}$		OC		EC		$PM_{2.5}$		OC		EC	
	c	%	*c*	%	*c*	%	*c*	%	*c*	%	*c*	%	*c*	%	*c*	%	*c*	%	*c*	%	*c*	%	*c*	%	*c*	%	*c*	%	*c*	%
Oil combustion	1.0	2.0	0.0	0.0	0.1	4.9	1.5	2.3	0.0	0.0	0.2	8.4	0.6	0.6	0.0	0.0	0.1	1.5	0.3	0.3	0.0	0.0	0.0	0.6	0.9	1.1	0.0	0.	0.1	2.8
Secondary nitrate	11.5	23.7	0.2	1.8	0.0	0.0	20.1	30.4	0.3	3.9	0.0	0.0	19.3	21.0	0.3	1.8	0.0.	0.0	17.4	14.4	0.2	1.1	0.0	0.0	17.0	20.8	0.2	1.8	0.0	0.0
Waste incineration	1.7	3.6	0.0	0.0	0.0	0.0	2.2	3.3	0.0	0.0	0.0	0.0	6.1	6.7	0.0	0.0	0.0	0.0	3.4	2.8	0.0	0.0	0.0	0.0	3.2	3.9	0.0	0.0	0.0	0.0
Dust	6.5	13.4	2.0	22.1	0.0	0.0	0.9	1.4	0.3	4.1	0.0	0.0	2.7	3.0	0.9	5.6	0.0	0.0	1.8	1.5	0.6	2.5	0.0	0.0	2.9	3.6	0.9	6.8	0.0	0.0
Secondary sulfate	5.4	11.2	0.3	3.8	0.0	0.0	20.0	30.3	1.3	17.8	0.0	0.0	15.2	16.5	1.0	6.3	0.0	0.0	33.5	27.8	2.1	9.7	0.0	0.0	19.1	23.3	1.2	9.1	0.0	0.0
Biomass burning	2.4	4.9	0.9	9.6	0.2	8.0	1.1	1.7	0.4	5.7	0.1	4.1	17.6	19.1	6.3	41.4	1.6	31.4	19.1	15.8	6.9	31.5	1.7	25.2	9.6	11.8	3.5	26.2	0.9	20.5
Coal combustion	3.8	7.8	0.3	3.4	0.3	10.2	7.0	10.6	0.6	7.9	0.5	20.1	11.2	12.1	0.9	5.8	0.8	15.8	11.9	9.9	1.0	4.4	0.8	12.5	8.4	10.2	0.7	5.0	0.6	14.1
Industry	1.5	3.0	0.0	0.0	0.3	11.7	1.1	1.7	0.0	0.0	0.2	10.1	3.0	2.4	0.0	0.0	0.6	11.9	2.4	2.0	0.0	0.0	0.5	7.8	1.9	2.3	0.0	0.0	0.4	9.8
Vehicle emissions	14.7	30.4	5.4	59.2	1.8	65.2	12.1	18.3	4.3	60.6	1.4	57.4	16.7	18.1	6.0	39.1	2.0	39.4	30.7	25.5	11.1	50.8	3.6	54.0	18.8	23.0	6.8	51.0	2.2	52.9

loading of OC; thus, the source was identified as secondary sulfate. OC accompanying SO_4^{2-} and NH_4^+ was attributed to SOC formation (Wong et al., 2019). Interestingly, 26.7% of Se was found in the secondary sulfate factor in this study. Our results are consistent with the findings of previous studies (Hao et al., 2020; Jeong et al., 2016; Weber et al., 2019). Similar to sulfur, Se originates primarily from coal combustion and has a removal rate similar to that of SO_4^{2-}; therefore, Se can be used to trace SO_2 oxidation in clouds and fog (Husain et al., 2004).

Factor 6 was characterized by high loadings of K, Cl^-, OC and EC, and the source was identified as biomass burning (Liu et al., 2019).

In factor 7, a high loading of arsenic (As) was observed, which is considered a reliable tracer of coal combustion (Cui et al., 2019; Liu et al., 2019); thus, this source could be identified as coal combustion. Additionally, approximately 20% of Se was also apportioned to coal combustion. Higher contributions of coal combustion to $PM_{2.5}$ were found in autumn and winter than in spring and summer (Table 2).

Factor 8 was heavily loaded with Cr and Mn. These metallic species can usually be used for tracking industrial sources (Liu et al., 2019; Xu et al., 2019a). Thus, the source could be identified as industrial emissions.

Factor 9 was characterized by high loadings of OC and EC. Previous studies have indicated that high contributions of OC and EC in $PM_{2.5}$ originate from vehicle emissions in Beijing (Liu et al., 2019; Xu et al., 2019a; Zíková et al., 2016). In addition, Cu and Zn were also found in this factor. As reported by the emission inventory of elements in Beijing (Zhu et al., 2018), brake and tire wear are sources of Cu in Beijing, accounting for approximately 68.4% of the total emission of Cu. Zn is added to tire treads to facilitate the vulcanization process. This factor contributed 23% of $PM_{2.5}$ on average. High correlations between the $PM_{2.5}$ concentrations from vehicle emissions and CO ($r^2 = 0.54$) or NO_x ($r^2 = 0.51$) also confirmed the contribution of vehicle emissions. This result is consistent with previous studies, which indicated that vehicle emissions contribute 20.8–24.9% of $PM_{2.5}$ in Beijing (Zíková et al., 2016; Huang et al., 2017; Xu et al., 2019a). In addition, the results of source apportionment based on hourly measurements of $PM_{2.5}$ and chemical compositions from November 7, 2016, to December 22, 2016, show that vehicular emissions contribute 18% of $PM_{2.5}$ (Liu et al., 2019), which is very close to the results during the autumn and winter seasons in this study. Vehicle emissions contributed 18.1% and 25.5% of $PM_{2.5}$ on average in the autumn and winter in this study, respectively.

3.4. Contribution of vehicle emissions to OC, EC and $PM_{2.5}$

To study the contribution of vehicle emissions to OC, EC and $PM_{2.5}$, the variations in and the evolution of OC, EC and $PM_{2.5}$ concentrations in factor 9 are discussed in detail based on the source profile identified by the PMF model. As presented in Table 2, the annual average traffic-related contributions to the measured OC and EC concentrations were 51.0% (6.8 μg/m^3) and 52.9% (2.2 μg/m^3), respectively. The annual average ratio of $OC_{vehicle}$ to $EC_{vehicle}$ was approximately 3.1, which is consistent with that of OC/EC emitted from gasoline vehicles (1.2–4.8) (Hao et al., 2019; Yang et al., 2019).

The diurnal variations in vehicle-associated OC, EC and $PM_{2.5}$ are shown in Fig. 7. It was obvious that OC, EC and $PM_{2.5}$ showed higher levels during the nighttime, MR and ER. As shown in Table 3 and Fig. 7, the annual average vehicle emissions contributed 51.2% (7.5 μg/m^3), 51.3% (2.5 μg/m^3) and 25.2% (20.9 μg/m^3) to OC, EC and $PM_{2.5}$ during the nighttime, respectively. The concentrations of vehicle emissions to OC, EC and $PM_{2.5}$ during the nighttime were also 14.7%, 16.0% and 14.4% higher than those during the MR, respectively, while they were 8.0%, 8.0% and 7.2% higher than those during the ER, respectively ($p > .05$). For the seasonal variations in the contribution from vehicle emissions to OC (Table 3), the concentrations during the nighttime were 13.8%, 15.6% and 23.8% higher than those during the MR in spring, summer and winter, respectively, while they were 33.8%, 8.9% and 2.4% higher than those during the ER in spring, summer and winter, respectively. For the concentrations of vehicle emissions to EC, the concentrations during the nighttime were 14.3%, 20.0% and 24.4% higher than those during the MR in spring, summer and winter, respectively, while they were 33.3%, 6.7% and 2.4% higher than those during the ER in spring, summer and winter, respectively. The concentrations of vehicle emissions to $PM_{2.5}$ during the nighttime were 12.9% 7.9% and 25.1% higher than those during the MR in spring, summer and winter, respectively, while they were 32.0%, 8.7% and 1.7% higher than those during the ER in spring, summer and winter, respectively. However, only the differences in the concentrations of OC, EC and $PM_{2.5}$ from vehicle emission during the nighttime and the ER in spring were significant ($p < .05$) based on the Mann-Whitney *U* test. Traffic-related OC, EC and $PM_{2.5}$ concentrations in the autumn and winter were higher than those in the spring and summer, which was likely related to the cold start of vehicles (Nam et al., 2010; Schauer et al., 2008).

Despite no obvious fluctuation in vehicle population in the four seasons, the seasonal difference was recorded in the concentrations and the contribution (%) of vehicle emissions to $PM_{2.5}$, OC and EC during the nighttime, MR and ER. Regarding the concentrations of vehicle emissions to $PM_{2.5}$, OC and EC during the nighttime, MR and ER, the lowest values occurred in summer, whereas the highest values occurred in winter. The Kruskal-Wallis test was used to determine the seasonal differences in the concentrations of vehicle emissions to $PM_{2.5}$, OC and EC during the nighttime, MR and ER, and significant differences were found ($p < .05$). The Dunn multiple-comparison test was further used to determine the pair-wise differences in the concentrations of vehicle emissions to $PM_{2.5}$, OC and EC during the nighttime, MR and ER in the four seasons. Notably, regarding the concentrations of vehicle emissions to $PM_{2.5}$, OC and EC, there were no significant differences between spring and autumn ($p > .05$) during the nighttime and MR, while no significant differences were found between spring and summer during the ER. As shown in Fig. S1, the high *T* not only lowers vehicle emissions of $PM_{2.5}$, OC and EC in summer (Nam et al., 2010; Schauer et al., 2008) but also facilitates semi-volatile compounds in the gas phase. Additionally, high *PBL* and frequent precipitation in summer are favorable for lowering the concentrations of $PM_{2.5}$, OC and EC from vehicle emissions. Thus, the lowest concentrations of vehicle emissions to $PM_{2.5}$, OC and EC occurred in summer. On the contrary, low *T* and low *PBL* resulted in the highest values in winter.

Although vehicle emissions resulted in higher concentrations of $PM_{2.5}$, OC and EC during the nighttime, MR and ER in autumn and winter, the lower contributions (%) of vehicle emissions to $PM_{2.5}$, OC and EC in autumn and winter were caused by the higher increment of other sources. For example, the higher contribution (%) of biomass burning to OC and EC in autumn (41.4% and 31.4% for OC and EC) and winter (31.5% and 25.2% for OC and EC) resulted in lower contribution of vehicle emissions during the nighttime, MR and ER in autumn and winter. Regarding the $PM_{2.5}$, the highest contributions (60.7%) of secondary sources (secondary sulfate and nitrate) in summer resulted in the lowest contribution of vehicle emissions to $PM_{2.5}$ in summer during the MR (16.8%) and ER (16.0%), while both the highest contribution (22.4%) of biomass burning and higher contributions (35.4%) of secondary sources during the nighttime resulted in the lowest contribution (17.5%) of vehicle emissions to $PM_{2.5}$ during the nighttime in autumn (Table 3). In contrast to the other seasons, the maximum contributions of vehicle emissions to $PM_{2.5}$ were recorded during the nighttime (34.2%), MR (29.0%) and ER (28.9%) in spring. Although the lowest *T* in winter increased the emissions of $PM_{2.5}$ from vehicles (Nam et al., 2010), higher contributions (66.1%) of secondary sources, coal combustion and biomass burning to $PM_{2.5}$ resulted in lower contributions of vehicle emissions to $PM_{2.5}$ during the nighttime, MR and ER in winter than in spring (Table 3).

The result in summer (60.6%) is similar to that reported by (Wang

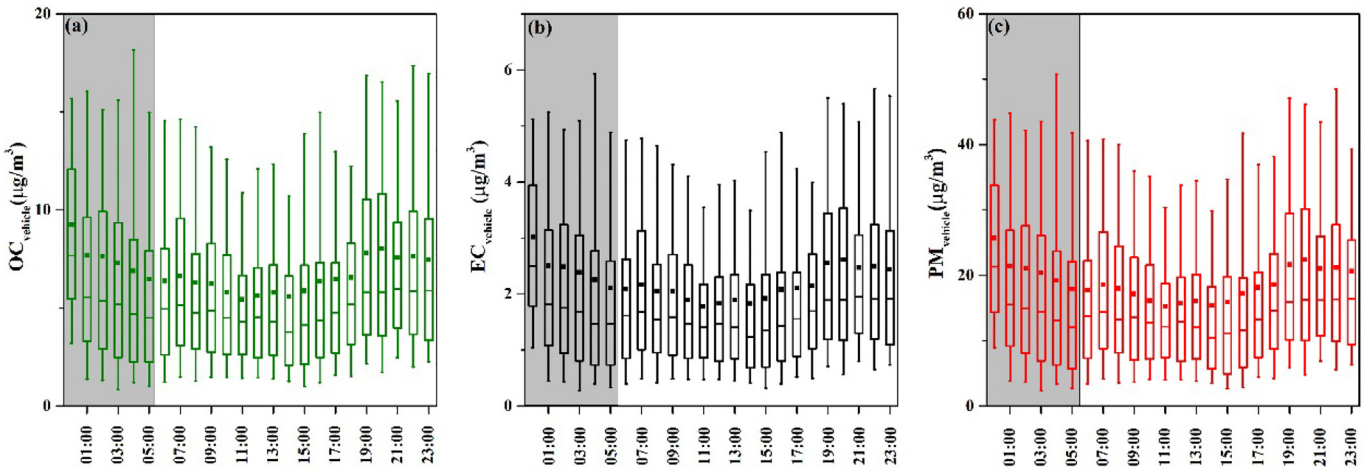

Fig. 7. Diurnal variation in the source contribution (μg/m^3) of vehicle emissions to (a) OC, (b) EC and (c) $PM_{2.5}$ (the shaded area represents the nighttime) (box length: 25th and 75th percentiles; whiskers: 10th and 90th percentiles; solid square in the box: mean; line in the box: median).

et al., 2015a), who found that vehicle emissions comprise 63.0% of OC in $PM_{2.5}$ using PCA in Beijing. Previous results based on radiocarbon (^{14}C) analysis and organic markers have shown that the relative contributions of vehicles to EC in both warm (March to October) and cold periods (November to February) are 79 ± 6% and 50 ± 7%, respectively (Zhang et al., 2015), which are consistent with the contributions of vehicle emissions to EC in warm (spring and summer, 57.4–65.2%) and cold (autumn and winter, 39.4–54.0%) periods in this study. Thus, the estimation of the contribution of vehicular emissions to carbonaceous aerosols is reasonable and reliable. Additionally, we also summarize the results regarding the contributions of vehicle emissions to OC and EC in cities in China and other countries in Table 4. As shown in Table 4, the results of the contributions of vehicle emissions to OC in this study are within the ranges of other cities (12.9–68%) in China (Al-Naiema et al., 2018; Huang et al., 2014; Wang et al., 2016a; Wei et al., 2019; Zheng et al., 2006) and those (23.8–87.2%) of other countries (Arhami et al., 2018; Green et al., 2013; Hamad et al., 2015; Heo et al., 2013; Perrone et al., 2012; Villalobos et al., 2015; Yin et al., 2010), while the results of the contributions of vehicle emissions to EC in this study are within the ranges of those (22–97%) in China (Al-Naiema et al., 2018; Wei et al., 2019; Zhang et al., 2015; Zhao et al., 2018) and lower than those (85.9–98.6%) of other countries (Green et al., 2013; Lambe et al., 2009; Yin et al., 2010). In summary, the percentages of contributions of vehicle emissions to OC, EC and $PM_{2.5}$ in this study were consistent with those in previous studies. Moreover, quantitative estimation of traffic-related contributions was obtained during the peak traffic periods, which was helpful to control traffic-related air pollution for policymakers or researchers and reduce the uncertainty concerning OC and EC emissions.

4. Conclusion

To estimate the contribution of vehicular emissions to OC, EC and $PM_{2.5}$, hourly concentrations of OC and EC in $PM_{2.5}$ were measured at an urban site in Beijing from June 1, 2016, to May 31, 2017, in addition to auxiliary measurements of $PM_{2.5}$-associated water-soluble ions and elements. The main conclusions are as follows.

(1) After excluding the influence of the *PBL* evolution, nighttime emission of HDDTs and HDVs resulted in higher levels of EC in contrast to those observed in the morning and evening rush hours, while the synergistic effect of vehicle emission, cooking activities and the secondary formation led to higher OC concentrations in the evening rush hours.
(2) Similar to cities in China and other countries, the average contributions of vehicles emissions to OC and EC were exceeded 50% in Beijing during the entire study period, suggesting that vehicle emissions are the most dominant sources of OC and EC in urban areas.
(3) During the nighttime, the contributions of emissions of HDVs and HDDTs to OC, EC and $PM_{2.5}$ were higher than or close to those during the morning and evening rush hours. More stringent emission standards of HDVs and HDDTs should be determined to further reduce OC, EC and even $PM_{2.5}$.

The aforementioned results indicated that the emissions of HDVs and HDDTs during the nighttime should be more concerned by policy makers and the scientific community. In future studies, measurements of organic tracers combined with analyses of traffic flow and type and driving speed will be helpful to apportion the contributions of different types of vehicles as well as to effectively control air pollution and

Table 3
Concentration (*c*, μg/m^3) and contribution (%) of vehicle emissions to $PM_{2.5}$, OC and EC in the four seasons during the nighttime (N), morning rush hours (MR) and evening rush hours (ER).

		Spring			Summer			Autumn			Winter			Year		
		N	MR	ER	N	MR	ER	N	MR	ER	N	MR	ER	N	MR	ER
OC	*c*	6.5	5.6	4.3	4.5	3.8	4.1	6.2	8.3	7.0	12.6	9.6	12.3	7.5	6.4	6.9
	%	62.0	55.7	58.7	66.2	58.8	55.8	35.8	47.0	43.8	50.9	49.4	52.7	51.2	50.4	52.0
EC	*c*	2.1	1.8	1.4	1.5	1.2	1.4	2.0	2.7	2.3	4.1	3.1	4.0	2.5	2.1	2.3
	%	64.3	59.3	71.0	59.0	49.6	57.7	34.8	48.7	44.7	52.9	51.7	56.7	51.3	50.9	55.8
$PM_{2.5}$	*c*	17.8	15.5	12.1	12.7	11.7	11.6	17.3	17.5	19.5	35.0	26.2	34.4	20.9	17.9	19.4
	%	34.2	29.0	28.9	23.7	16.8	16.0	17.5	21.2	18.9	26.7	25.3	25.3	25.2	23.1	22.2

Table 4
Contributions (%) of vehicle emissions to OC and EC in $PM_{2.5}$ in several cities in China and other countries.

Site	Site type	Period	Method	OC	EC	Reference
Beijing, China	Urban	Jun. 1, 2016 to May 31, 2017	PMF	51.0%	52.9%	This study
Beijing, China	Urban	Summer, 2016	PMF	60.6%	57.4%	This study
Beijing, China	Urban	Autumn, 2016	PMF	39.1%	39.4%	This study
Beijing, China	Urban	Winter, 2016	PMF	50.8%	54.0%	This study
Beijing, China	Urban	Spring, 2017	PMF	59.2%	65.2%	This study
Beijing, China	Urban	Warm period, 2010–2011	Radiocarbon (^{14}C) and organic marker	–	79%	Zhang et al. (2015)
Beijing, China	Urban	Cold period, 2010–2011	Radiocarbon (^{14}C) and organic marker	–	50%	Zhang et al. (2015)
Beijing, China	Urban	Summer, 2012	PCA	63%	–	Wang et al. (2015a)
Tangshan, China	Urban	Summer, 2012	PCA	45.2%	–	Wang et al. (2015a)
Shenzhen, China	Urban	Summer, 2011	CMB	23.2%–58.3%	93%–97%	Al-Naiema et al. (2018)
Xi'an, China	Urban	Jul. 2008 to Jun. 2009	Stable carbon isotopes	–	47%	Zhao et al. (2018)
Xi'an, China	Urban	Spring	Stable carbon isotopes	–	62%	Zhao et al. (2018)
Xi'an, China	Urban	Summer	Stable carbon isotopes	–	61%	Zhao et al. (2018)
Xi'an, China	Urban	Autumn	Stable carbon isotopes	–	57%	Zhao et al. (2018)
Xi'an, China	Urban	Winter	Stable carbon isotopes	–	22%	Zhao et al. (2018)
Guangzhou, China	Urban	Winter, 2012	CMB	15.3%	–	Wang et al. (2016a)
Guangzhou, China	Urban	Summer, 2012	CMB	12.9%	–	Wang et al. (2016a)
Shanghai, China	Urban	Winter, 2013	Stable carbon isotopes	–	54%	Wei et al. (2019)
Hong Kong, China	Roadside	Dec. 2000 to Oct. 2001	CMB	68%	–	Zheng et al. (2006)
Hong Kong, China	Urban	Dec. 2000 to Oct. 2001	CMB	60%	–	Zheng et al. (2006)
Hong Kong, China	Roadside	May 2011 to Apr. 2012	PMF	17%–64%	–	Huang et al. (2014)
Tehran, Iran	Urban	Feb. 2014 to Feb. 2015	CMB	72%	–	Arhami et al. (2018)
Santiago, Chile	Urban	Mar. to Oct. 2013	CMB	33.7%	–	Villalobos et al. (2015)
Baghdad, Iraq	Urban	Sep. 2012 to Sep. 2013	CMB	54%	–	Hamad et al. (2015)
Los Angeles, USA	Urban	May 2009 to Apr.2010	PMF	28%	–	Heo et al. (2013)
Las Vegas Valley, USA	Urban	Jan., 2003	CMB	75.1%–87.2%	85.9%–94.3%	Green et al. (2013)
Milan, Italy	Urban	Spring, 2006–2009	CMB	38%	–	Perrone et al. (2012)
Milan, Italy	Urban	Summer, 2006–2009	CMB	63%	–	Perrone et al. (2012)
Milan, Italy	Urban	Autumn, 2006–2009	CMB	52%	–	Perrone et al. (2012)
Milan, Italy	Urban	Winter, 2006–2009	CMB	48%	–	Perrone et al. (2012)
Pittsburgh, USA	Urban	Feb. to Apr., 2008	PMF	–	87%	Lambe et al. (2009)
Birmingham, UK	Urban	May 2007 to Apr. 2008	CMB	23.8%	98.6%	Yin et al. (2010)

reduce human health impacts caused by vehicles in Beijing.

Declaration of Competing Interest

The authors declare that they have no known competing financial interests or personal relationships that could have appeared to influence the work reported in this paper.

Acknowledgement

This work was supported by the National Key Research and Development Program of China (Grant No. 2017YFC0210000) and the CAS Key Technology Talent Program (Grant No. 1708). The authors would like to thank all members of the LAPC/CERN in IAP, CAS, for maintaining the instruments used in the current study.

Appendix A. Supplementary data

Supplementary data to this article can be found online at https://doi.org/10.1016/j.atmosres.2020.105153.

References

Al-Naiema, I.M., Yoon, S., Wang, Y.-Q., Zhang, Y.-X., Sheesley, R.J., Stone, E.A., 2018. Source apportionment of fine particulate matter organic carbon in Shenzhen, China by chemical mass balance and radiocarbon methods. Environ. Pollut. 240, 34–43.

Arhami, M., Shahne, M.Z., Hosseini, V., Haghighat, N.R., Lai, A.M., Schauer, J.J., 2018. Seasonal trends in the composition and sources of $PM_{2.5}$ and carbonaceous aerosol in Tehran, Iran. Environ. Pollut. 239, 69–81.

Belis, C.A., Karagulian, F., Larsen, B.R., Hopke, P.K., 2013. Critical review and meta-analysis of ambient particulate matter source apportionment using receptor models in Europe. Atmos. Environ. 69, 94–108.

Biswas, S., Verma, V., Schauer, J.J., Cassee, F.R., Cho, A.K., Sioutas, C., 2009. Oxidative potential of semi-volatile and non volatile particulate matter (PM) from heavy-duty vehicles retrofitted with emission control technologies. Environ. Sci. Technol. 43, 3905–3912.

Bond, T.C., Doherty, S.J., Fahey, D.W., Forster, P.M., Berntsen, T., DeAngelo, B.J., Flanner, M.G., Ghan, S., Kärcher, B., Koch, D., 2013. Bounding the role of black carbon in the climate system: a scientific assessment. J. Geophys. Res. Atmos. 118, 5380–5552.

Bressi, M., Sciare, J., Ghersi, V., Bonnaire, N., Nicolas, J.B., Petit, J.E., Moukhtar, S., Rosso, A., Mihalopoulos, N., Féron, A., 2013. A one-year comprehensive chemical characterisation of fine aerosol ($PM_{2.5}$) at urban, suburban and rural background sites in the region of Paris (France). Atmos. Chem. Phys. 13, 7825–7844.

Briggs, N.L., Long, C.M., 2016. Critical review of black carbon and elemental carbon source apportionment in Europe and the United States. Atmos. Environ. 144, 409–427.

Chang, Y., Deng, C., Cao, F., Cao, C., Zou, Z., Liu, S., Lee, X., Li, J., Zhang, G., Zhang, Y., 2017. Assessment of carbonaceous aerosols in Shanghai, China – part 1: long-term evolution, seasonal variations, and meteorological effects. Atmos. Chem. Phys. 17, 9945–9964.

Chen, Y., Xie, S.D., Luo, B., Zhai, C.Z., 2017. Particulate pollution in urban Chongqing of Southwest China: Historical trends of variation, chemical characteristics and source apportionment. Sci. Total Environ. 584, 523–534.

Cui, Y., Ji, D.S., Chen, H., Gao, M., Maenhaut, W., He, J., Wang, Y.S., 2019. Characteristics and sources of hourly trace elements in airborne fine particles in urban Beijing, China. J. Geophys. Res. Atmos. 124, 11,595–11,613.

Cui, Y., Ji, D.S., He, J., Kong, S.F., Wang, Y.S., 2020. In situ continuous observation of hourly elements in $PM_{2.5}$ in urban Beijing, China: occurrence levels, temporal variation, potential source regions and health risks. Atmos. Environ. 222, 117164.

Flores, R.M., Mertoğlu, E., Özdemir, H., Akkoyunlu, B.O., Demir, G., Ünal, A., Tayanç, M., 2020. A high-time resolution study of $PM_{2.5}$, organic carbon, and elemental carbon at an urban traffic site in Istanbul. Atmos. Environ. 223, 117241.

Gao, J., Peng, X., Chen, G., Xu, J., Shi, G.L., Zhang, Y.C., Feng, Y.C., 2016. Insights into the chemical characterization and sources of $PM_{2.5}$ in Beijing at a 1-h time resolution. Sci. Total Environ. 542, 162–171.

Gao, J., Woodward, A., Vardoulakis, S., Kovats, S., Wilkinson, P., Li, L., Xu, L., Li, J., Yang, J., Li, J., Cao, L., Liu, X., Wu, H., Liu, Q., 2017. Haze, public health and mitigation measures in China: a review of the current evidence for further policy response. Sci. Total Environ. 578, 148–157.

Green, M.C., Chow, J.C., Chang, M.-C.O., Chen, L.-W.A., Kuhns, H.D., Etyemezian, V.R., Watson, J.G., 2013. Source apportionment of atmospheric particulate carbon in Las Vegas, Nevada, USA. Particuology 11, 110–118.

Hamad, S.H., Schauer, J.J., Heo, J., Kadhim, A.K., 2015. Source apportionment of $PM_{2.5}$ carbonaceous aerosol in Baghdad, Iraq. Atmos. Res. 156, 80–90.

Han, S., Kondo, Y., Oshima, N., Takegawa, N., Miyazaki, Y., Hu, M., Lin, P., Deng, Z., Zhao, Y., Sugimoto, N., 2009. Temporal variations of elemental carbon in Beijing. J. Geophys. Res. Atmos. 114.

Hao, Y., Gao, C., Deng, S., Yuan, M., Song, W., Lu, Z., Qiu, Z., 2019. Chemical characterisation of $PM_{2.5}$ emitted from motor vehicles powered by diesel, gasoline,

natural gas and methanol fuel. Sci. Total Environ. 674, 128–139.
Hao, Y., Meng, X., Yu, X., Lei, M., Li, W., Yang, W., Shi, F., Xie, S., 2020. Quantification of primary and secondary sources to $PM_{2.5}$ using an improved source regional apportionment method in an industrial city, China. Sci. Total Environ. 706, 135715.
Heo, J., Dulger, M., Olson, M.R., McGinnis, J.E., Shelton, B.R., Matsunaga, A., Sioutas, C., Schauer, J.J., 2013. Source apportionments of $PM_{2.5}$ organic carbon using molecular marker positive Matrix Factorization and comparison of results from different receptor models. Atmos. Environ. 73, 51–61.
Hu, D., Bian, Q., Lau, A.K., Yu, J.Z., 2010. Source apportioning of primary and secondary organic carbon in summer $PM_{2.5}$ in Hong Kong using positive matrix factorization of secondary and primary organic tracer data. J. Geophys. Res. Atmos. 115.
Huang, X., Liu, Z., Liu, J., Hu, B., Wen, T., Tang, G., Zhang, J., Wu, F., Ji, D., Wang, L., Wang, Y., 2017. Chemical characterization and source identification of PM2.5 at multiple sites in the Beijing–Tianjin–Hebei region, China. Atmos. Chem. Phys. 17, 12941–12962.
Huang, K., Zhuang, G., Lin, Y., Wang, Q., Fu, J.S., Zhang, R., Li, J., Deng, C., Fu, Q., 2012. Impact of anthropogenic emission on air quality over a megacity–revealed from an intensive atmospheric campaign during the Chinese Spring Festival. Atmos. Chem. Phys. 12, 11631–11645.
Huang, X.H.H., Bian, Q.J., Louie, P.K.K., Yu, J.Z., 2014. Contributions of vehicular carbonaceous aerosols to $PM_{2.5}$ in a roadside environment in Hong Kong. Atmos. Chem. Phys. 14, 9279–9293.
Husain, L., Ghauri, B., Yang, K., Khan, A.R., Rattigan, O., 2004. Application of the SO_4^{2-}/Se tracer technique to study SO_2 oxidation in cloud and fog on a time scale of minutes. Chemosphere 54, 177–183.
Jeong, C.-H., Wang, J.M., Evans, G.J., 2016. Source Apportionment of Urban Particulate Matter using Hourly Resolved Trace Metals, Organics, and Inorganic Aerosol Components. Atmo. Chem. Phys. Discus. 1–32.
Ji, D., Gao, W., Zhang, J., Morino, Y., Zhou, L., Yu, P., Li, Y., Sun, J., Ge, B., Tang, G., Sun, Y., Wang, Y., 2016a. Investigating the evolution of summertime secondary atmospheric pollutants in urban Beijing. Sci. Total Environ. 572, 289–300.
Ji, D., Zhang, J.K., He, J., Wang, X.J., Pang, B., Liu, Z.R., Wang, L.L., Wang, Y.S., 2016b. Characteristics of atmospheric organic and elemental carbon aerosols in urban Beijing, China. Atmos. Environ. 125, 293–306.
Ji, D., Gao, M., Maenhaut, W., He, J., Wu, C., Cheng, L.J., Gao, W.K., Sun, Y., Sun, J.R., Xin, J.Y., 2019a. The carbonaceous aerosol levels still remain a challenge in the Beijing-Tianjin-Hebei region of China: Insights from continuous high temporal resolution measurements in multiple cities. Environ. Int. 126, 171–183.
Ji, D., Gao, W.K., Maenhaut, W., He, J., Wang, Z., Li, J.W., Du, W.P., Wang, L.L., Sun, Y., Xin, J.Y., 2019b. Impact of air pollution control measures and regional transport on carbonaceous aerosols in fine particulate matter in urban Beijing, China: insights gained from long-term measurement. Atmos. Chem. Phys. 19, 8569–8590.
Lambe, A.T., Logue, J.M., Kreisberg, N.M., Hering, S.V., Worton, D.R., Goldstein, A.H., Donahue, N.M., Robinson, A.L., 2009. Apportioning black carbon to sources using highly time-resolved ambient measurements of organic molecular markers in Pittsburgh. Atmos. Environ. 43, 3941–3950.
Li, C., Chen, P., Kang, S., Yan, F., Hu, Z., Qu, B., Sillanpää, M., 2016a. Concentrations and light absorption characteristics of carbonaceous aerosol in $PM_{2.5}$ and PM_{10} of Lhasa city, the Tibetan Plateau. Atmos. Environ. 127, 340–346.
Li, H., Guo, L., Cao, R., Gao, B., Yan, Y., He, Q., 2016b. A wintertime study of $PM_{2.5}$-bound polycyclic aromatic hydrocarbons in Taiyuan during 2009–2013: Assessment of pollution control strategy in a typical basin region. Atmos. Environ. 140, 404–414.
Li, L., Tan, Q., Zhang, Y., Feng, M., Qu, Y., An, J., Liu, X., 2017. Characteristics and source apportionment of $PM_{2.5}$ during persistent extreme haze events in Chengdu, Southwest China. Environ. Pollut. 230, 718–729.
Lin, P., Hu, M., Deng, Z., Slanina, J., Han, S., Kondo, Y., Takegawa, N., Miyazaki, Y., Zhao, Y., Sugimoto, N., 2009. Seasonal and diurnal variations of organic carbon in $PM_{2.5}$ in Beijing and the estimation of secondary organic carbon. J. Geophys. Res. Atmos. 114.
Liu, B., Wu, J., Zhang, J., Wang, L., Yang, J., Liang, D., Dai, Q., Bi, X., Feng, Y., Zhang, Y., Zhang, Q., 2017a. Characterization and source apportionment of $PM_{2.5}$ based on error estimation from EPA PMF 5.0 model at a medium city in China. Environ. Pollut. 222, 10–22.
Liu, B., Yang, J., Yuan, J., Wang, J., Dai, Q., Li, T., Bi, X., Feng, Y., Xiao, Z., Zhang, Y., Xu, H., 2017b. Source apportionment of atmospheric pollutants based on the online data by using PMF and ME2 models at a megacity, China. Atmos. Res. 185, 22–31.
Liu, H., Wu, B., Liu, S., Shao, P., Liu, X., Zhu, C., Wang, Y., Wu, Y., Xue, Y., Gao, J., 2018. A regional high-resolution emission inventory of primary air pollutants in 2012 for Beijing and the surrounding five provinces of North China. Atmos. Environ. 181, 20–33.
Liu, Y., Zheng, M., Yu, M., Cai, X., Du, H., Li, J., Zhou, T., Yan, C., Wang, X., Shi, Z., Harrison, R.M., Zhang, Q., He, K., 2019. High-time-resolution source apportionment of $PM_{2.5}$ in Beijing with multiple models. Atmos. Chem. Phys. 19, 6595–6609.
Nam, E., Kishan, S., Baldauf, R.W., Fulper, C.R., Warila, J., 2010. Temperature effects on particulate matter emissions from light-duty, gasoline-powered motor vehicles. Environ. Sci. Technol. 44, 4672–4677.
Paatero, P., Tapper, U., 1994. Positive matrix factorization: a non-negative factor model with optimal utilization of error estimates of data values. Environmetrics 5, 111–126.
Park, S.S., Lee, K.-H., Kim, Y.J., Kim, T.Y., Cho, S.Y., Kim, S.J., 2008. High time-resolution measurements of carbonaceous species in $PM_{2.5}$ at an urban site of Korea. Atmos. Res. 89, 48–61.
Park, M.-B., Lee, T.-J., Lee, E.-S., Kim, D.-S., 2019. Enhancing source identification of hourly $PM_{2.5}$ data in Seoul based on a dataset segmentation scheme by positive matrix factorization (PMF). Atmos. Pollut. Res. 10, 1042–1059.
Pereira, G.M., Teinilä, K., Custódio, D., Gomes Santos, A., Xian, H., Hillamo, R., Alves, C.A., Bittencourt de Andrade, J., Olímpio da Rocha, G., Kumar, P., Balasubramanian, R., Andrade, M.d.F., de Castro Vasconcellos, P., 2017. Particulate pollutants in the Brazilian city of São Paulo: 1-year investigation for the chemical composition and source apportionment. Atmos. Chem. Phys. 17, 11943–11969.
Perrone, M., Larsen, B., Ferrero, L., Sangiorgi, G., De Gennaro, G., Udisti, R., Zangrando, R., Gambaro, A., Bolzacchini, E., 2012. Sources of high $PM_{2.5}$ concentrations in Milan, Northern Italy: molecular marker data and CMB modelling. Sci. Total Environ. 414, 343–355.
Pongpiachan, S., Kositanont, C., Palakun, J., Liu, S., Ho, K.F., Cao, J., 2015. Effects of day-of-week trends and vehicle types on $PM_{2.5}$-bounded carbonaceous compositions. Sci. Total Environ. 532, 484–494.
Pui, D.Y.H., Chen, S.-C., Zuo, Z., 2014. $PM_{2.5}$ in China: Measurements, sources, visibility and health effects, and mitigation. Particuology 13, 1–26.
Schauer, J.J., Christensen, C.G., Kittelson, D.B., Johnson, J.P., Watts, W.F., 2008. Impact of Ambient Temperatures and Driving Conditions on the Chemical Composition of Particulate Matter Emissions from Non-smoking Gasoline-Powered Motor Vehicles. Aerosol Sci. Technol. 42, 210–223.
Sharma, S., Mandal, T., 2017. Chemical composition of fine mode particulate matter ($PM_{2.5}$) in an urban area of Delhi, India and its source apportionment. Urban Clim. 21, 106–122.
Sofowote, U.M., Rastogi, A.K., Debosz, J., Hopke, P.K., 2014. Advanced receptor modeling of near–real–time, ambient $PM_{2.5}$ and its associated components collected at an urban–industrial site in Toronto, Ontario. Atmos. Pollut. Res. 5, 13–23.
Sun, Y., Xu, W., Zhang, Q., Jiang, Q., Canonaco, F., Prévôt, A.S.H., Fu, P., Li, J., Jayne, J., Worsnop, D.R., Wang, Z., 2018. Source apportionment of organic aerosol from 2-year highly time-resolved measurements by an aerosol chemical speciation monitor in Beijing, China. Atmos. Chem. Phys. 18, 8469–8489.
Tao, J., Zhang, L., Cao, J., Zhong, L., Chen, D., Yang, Y., Chen, D., Chen, L., Zhang, Z., Wu, Y., Xia, Y., Ye, S., Zhang, R., 2017. Source apportionment of $PM_{2.5}$ at urban and suburban areas of the Pearl River Delta region, South China - with emphasis on ship emissions. Sci. Total Environ. 574, 1559–1570.
Teetor, P., 2011. R cookbook: Proven Recipes for Data Analysis, Statistics, and Graphics. O'Reilly Media, Inc..
Villalobos, A.M., Barraza, F., Jorquera, H., Schauer, J.J., 2015. Chemical speciation and source apportionment of fine particulate matter in Santiago, Chile, 2013. Sci. Total Environ. 512, 133–142.
Wang, G., Cheng, S., Li, J., Lang, J., Wen, W., Yang, X., Tian, L., 2015a. Source apportionment and seasonal variation of $PM_{2.5}$ carbonaceous aerosol in the Beijing-Tianjin-Hebei region of China. Environ. Monit. Assess. 187, 143.
Wang, P., Cao, J.J., Shen, Z.X., Han, Y.M., Lee, S.C., Huang, Y., Zhu, C.S., Wang, Q.Y., Xu, H.M., Huang, R.J., 2015b. Spatial and seasonal variations of $PM_{2.5}$ mass and species during 2010 in Xi'an, China. Sci. Total Environ. 508, 477–487.
Wang, J., Ho, S.S.H., Ma, S., Cao, J., Dai, W., Liu, S., Shen, Z., Huang, R., Wang, G., Han, Y., 2016a. Characterization of $PM_{2.5}$ in Guangzhou, China: uses of organic markers for supporting source apportionment. Sci. Total Environ. 550, 961–971.
Wang, Y., Jia, C., Tao, J., Zhang, L., Liang, X., Ma, J., Gao, H., Huang, T., Zhang, K., 2016b. Chemical characterization and source apportionment of $PM_{2.5}$ in a semi-arid and petrochemical-industrialized city, Northwest China. Sci. Total Environ. 573, 1031–1040.
Wang, Y., Zhang, Y., Schauer, J.J., de Foy, B., Guo, B., Zhang, Y., 2016c. Relative impact of emissions controls and meteorology on air pollution mitigation associated with the Asia-Pacific Economic Cooperation (APEC) conference in Beijing, China. Sci. Total Environ. 571, 1467–1476.
Weber, S., Salameh, D., Albinet, A., Alleman, L.Y., Waked, A., Besombes, J.-L., Jacob, V., Guillaud, G., Meshbah, B., Rocq, B., 2019. Comparison of PM_{10} sources profiles at 15 French Sites using a Harmonized constrained positive matrix factorization approach. Atmosphere 10, 310.
Wei, N., Xu, Z., Wang, G., Liu, W., Zhouga, D., Xiao, D., Yao, J., 2019. Source apportionment of carbonaceous aerosols during haze days in Shanghai based on dual carbon isotopes. J. Radioanal. Nucl. Chem. 321, 383–389.
Zhu, C., Tian, H., Hao, Y., Gao, J., Hao, J., Wang, Y., Hua, S., Wang, K., Liu, H., 2018. A high-resolution emission inventory of anthropogenic trace elements in Beijing-Tianjin-Hebei (BTH) region of China. Atmos. Environ. 191, 452–462.
Wong, Y.K., Huang, X.H., Cheng, Y.Y., Louie, P.K., Alfred, L., Tang, A.W., Chan, D.H., Yu, J.Z., 2019. Estimating contributions of vehicular emissions to $PM_{2.5}$ in a roadside environment: a multiple approach study. Sci. Total Environ. 672, 776–788.
Wu, B., Shen, X., Cao, X., Yao, Z., Wu, Y., 2016. Characterization of the chemical composition of PM2.5 emitted from on-road China III and China IV diesel trucks in Beijing, China. Sci. Total Environ. 551, 579–589.
Wu, C., Wu, D., Yu, J.Z., 2019. Estimation and uncertainty Analysis of secondary Organic Carbon using 1 year of Hourly Organic and Elemental Carbon Data. J. Geophys. Res. Atmos. 124, 2774–2795.
Xie, S., Liu, Z., Chen, T., Hua, L., 2008. Spatiotemporal variations of ambient PM_{10} source contributions in Beijing in 2004 using positive matrix factorization. Atmos. Chem. Phys. 8, 2701–2716.
Xu, H., Xiao, Z., Chen, K., Tang, M., Zheng, N., Li, P., Yang, N., Yang, W., Deng, X., 2019a. Spatial and temporal distribution, chemical characteristics, and sources of ambient particulate matter in the Beijing-Tianjin-Hebei region. Sci. Total Environ. 658, 280–293.
Xu, W., Sun, Y., Wang, Q., Zhao, J., Wang, J., Ge, X., Xie, C., Zhou, W., Du, W., Li, J., 2019b. Changes in Aerosol Chemistry from 2014 to 2016 in Winter in Beijing: insights from high-resolution aerosol mass spectrometry. J. Geophys. Res. Atmos. 124, 1132–1147.
Yan, H., Wu, Y., Zhang, S., Song, S., Fu, L., Hao, J., 2014. Emission characteristics and concentrations of vehicular black carbon in a typical freeway traffic environment of Beijing. Acta Sci. Circumst. 34, 1891–1899.
Yang, H.-H., Dhital, N.B., Wang, L.-C., Hsieh, Y.-S., Lee, K.-T., Hsu, Y.-T., Huang, S.-C., 2019. Chemical characterization of fine particulate matter in gasoline and diesel

vehicle exhaust. Aerosol Air Qual. Res. 19, 1439–1449.
Yao, L., Huo, J., Wang, D., Fu, Q., Sun, W., Li, Q., Chen, J., 2020. Online measurement of carbonaceous aerosols in suburban Shanghai during winter over a three-year period: Temporal variations, meteorological effects, and sources. Atmos. Environ. 226, 117408.
Yin, J., Harrison, R.M., Chen, Q., Rutter, A., Schauer, J.J., 2010. Source apportionment of fine particles at urban background and rural sites in the UK atmosphere. Atmos. Environ. 44, 841–851.
Zhang, Y., Sheesley, R.J., Schauer, J.J., Lewandowski, M., Jaoui, M., Offenberg, J.H., Kleindienst, T.E., Edney, E.O., 2009. Source apportionment of primary and secondary organic aerosols using positive matrix factorization (PMF) of molecular markers. Atmos. Environ. 43, 5567–5574.
Zhang, Y.-L., Schnelle-Kreis, J.r., Abbaszade, G.l., Zimmermann, R., Zotter, P., Shen, R.-r., Schäfer, K., Shao, L., Prévôt, A.S., Szidat, S.n., 2015. Source apportionment of elemental carbon in Beijing, China: insights from radiocarbon and organic marker measurements. Environ. Sci. Technol. 49, 8408–8415.
Zhang, N., Han, B., He, F., Xu, J., Zhao, R., Zhang, Y., Bai, Z., 2017. Chemical characteristic of $PM_{2.5}$ emission and inhalational carcinogenic risk of domestic Chinese cooking. Environ. Pollut. 227, 24–30.
Zhao, P., Dong, F., Yang, Y., He, D., Zhao, X., Zhang, W., Yao, Q., Liu, H., 2013. Characteristics of carbonaceous aerosol in the region of Beijing, Tianjin, and Hebei, China. Atmos. Environ. 71, 389–398.
Zhao, Z., Cao, J., Zhang, T., Shen, Z., Ni, H., Tian, J., Wang, Q., Liu, S., Zhou, J., Gu, J., 2018. Stable carbon isotopes and levoglucosan for $PM_{2.5}$ elemental carbon source apportionments in the largest city of Northwest China. Atmos. Environ. 185, 253–261.
Zhao, Y., Chen, C., Zhao, B., 2019. Emission characteristics of $PM_{2.5}$-bound chemicals from residential Chinese cooking. Build. Environ. 149, 623–629.
Zheng, M., Hagler, G.S., Ke, L., Bergin, M.H., Wang, F., Louie, P.K., Salmon, L., Sin, D.W., Yu, J.Z., Schauer, J.J., 2006. Composition and sources of carbonaceous aerosols at three contrasting sites in Hong Kong. J. Geophys. Res. Atmos. 111.
Zíková, N., Wang, Y., Yang, F., Li, X., Tian, M., Hopke, P.K., 2016. On the source contribution to Beijing $PM_{2.5}$ concentrations. Atmos. Environ. 134, 84–95.